

# Space-time sensors using multiple-wave atom interferometry

F. Impens<sup>1,2</sup> and Ch. J. Bordé<sup>1,3</sup>

<sup>1</sup> SYRTE, Observatoire de Paris, 61 avenue de l'Observatoire, 75014 Paris, France

<sup>2</sup> Instituto de Física, Universidade Federal do Rio de Janeiro. Caixa Postal 68528, 21941-972 Rio de Janeiro, RJ, Brasil and

<sup>3</sup> Laboratoire de Physique des Lasers, Institut Galilée, F-93430 Villetaneuse, France

(Dated: July 19, 2022)

We propose a space-time sensor based on a succession of levitating Bordé-Ramsey interferometers set in a vertical configuration. The sample is coherently trapped in the longitudinal momentum space thanks to a multiple wave interference phenomenon. The system constitutes a matter-wave resonator in momentum space, whose set of resonance conditions yields a promising sensitivity in both the inertial and the frequency domain.

PACS numbers: 06.30.Ft, 06.30.Gv, 37.25.+k, 03.75.Dg, 42.50.Ct

Optical clocks have become frequency standards of high fractional accuracy, currently of the order of  $10^{-16}$  [1], and are as such promising tools to investigate basics physics through a battery of fundamental tests [2]. Horizontal Bordé-Ramsey interferometers [3, 4] have been used successfully to build atomic optical clocks of high stability [5]. However, in presence of gravity, this system presents two drawbacks: curvature shifts resulting from the transverse field profile exploration by the traveling atoms and a finite interrogation time [6]. This has led the metrology community to privilege experiments built around atomic traps [7], able to keep the sample in the Lamb-Dicke regime, thereby reducing residual shifts due to atomic motion and increasing the interaction time with the interrogation field. This paper proposes instead to circumvent the previous limitations with a multiple-wave atom interferometer [8], which rests on a succession of vertical Bordé-Ramsey interferometers. The usual sequence of two pairs of  $\pi/2$  pulses with inverted wave-vectors is here directed vertically, thus providing a net vertical momentum transfer to the atoms. The repetition of this sequence, assorted to a set of resonance conditions, gives rise to a levitation of the atomic sample. Field curvature effects are reduced by the system geometry, in which the laser beam and sample propagation axes coincide. Numerical simulations confirm that a fast central fringe narrowing occurs when the atomic sample is interrogated over several bounces, and that the multiple wave interference preserve the atomic population in levitation. Beyond seducing experimental features for frequency metrology, this system exhibits a special physical effect, which is the coherent localization of an atomic sample in momentum through a constructive multiple wave interference process. This motivates an analogy with an atomic Fabry-Perot resonator [9] in momentum space. This setup, derived from an earlier gravimeter proposal [10], has been presented in a number of conferences [11].

Let us begin by considering a simple yet important point illustrated on Fig. 1: when is a sequence of two distinct  $\pi/2$  pulses equivalent to a single  $\pi$  pulse? The answer to this question, not as trivial as it seems, is essential for Ramsey interferometry and also for our

system, which rests on a controlled momentum transfer through a sequence of  $\pi/2$  pulses. We consider a diluted

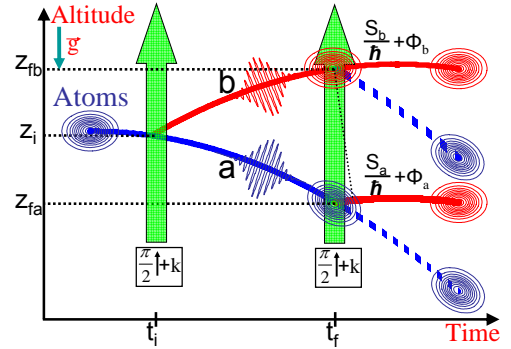


FIG. 1: Action of two distinct  $\pi/2$  pulses on a free-falling atomic wave-packet. The phase difference between the two outgoing wave-packets comes from the classical action and laser phase acquired on each path, and from the distance of their centers.

sample of two-level atoms evolving in the gravity field (considered as uniform) according to the Hamiltonian  $H = \frac{p^2}{2m} + mgz$ , initially in the lower state  $a$  and described by the Gaussian wave-function [12]  $\psi_a(\mathbf{r}, t_0) = \frac{\pi^{-3/2}}{\sqrt{w_{x0}w_{y0}w_{z0}}} e^{-\frac{m}{2\hbar} \left( \frac{(x-x_i)^2}{w_{x0}^2} + \frac{(y-y_i)^2}{w_{y0}^2} + \frac{(z-z_i)^2}{w_{z0}^2} \right) + \frac{i}{\hbar} \mathbf{p}_{ia}(t_0) \cdot (\mathbf{r} - \mathbf{r}_i)}$ . After the two  $\pi/2$  light pulses, performed at times  $t_i$  and  $t_f = t_i + T$ , the initial wave-packet has been split into four packets following two possible intermediate trajectories. The excited wave-function receives two wave-packet contributions coming from either path and associated with the absorption of a photon at times  $t_i$  and  $t_f$ , of common central momentum  $\mathbf{p}_f = \mathbf{p}_i + \hbar\mathbf{k} - m\mathbf{g}T$  and respective central positions  $\mathbf{r}_{fa}$  and  $\mathbf{r}_{fb}$ . On each path, these wave-packets acquire an action phase  $S_{a,b}/\hbar$  and a laser phase  $\phi_{a,b}$  evaluated at their center and at the corresponding interaction time. Both contributions to the excited state are phase-matched if the following relation is verified [13]:

$$-\mathbf{p}_f \cdot \mathbf{r}_{f,a} + S_a + \hbar\phi_a = -\mathbf{p}_f \cdot \mathbf{r}_{f,b} + S_b + \hbar\phi_b \quad (1)$$

The action and laser phases read respectively  $S_{a,b} = mg^2T^3/3 - \mathbf{p}_{ia,ib} \cdot \mathbf{g}T^2 + (p_{ia,ib}^2/2m - mgz_i - E_{a,b})T$  and  $\phi_{a,b} = \mathbf{k} \cdot \mathbf{r}_{i,fa} - \omega_{1,2}(t_{i,f} - t_c) + \phi_{1,2}^0$ . We have introduced the initial central momentum along the excited path  $\mathbf{p}_{ib} = \mathbf{p}_{ia} + \hbar\mathbf{k}$ , and the central time  $t_c = (t_i + t_f)/2$  used as phase reference for the two pulses. The terms  $\mathbf{p}_f \cdot \mathbf{r}_{fa,b}$  reflect the atom-optical path difference between both wave-packets at their respective centers. Condition (1) is fulfilled if the laser frequencies  $\omega_{1,2}$  are set to their resonant values

$$\omega_{1,2} = \frac{1}{\hbar} \left( E_b + \frac{(\mathbf{p}_{1,2} + \hbar\mathbf{k})^2}{2m} - E_a - \frac{p_{1,2}^2}{2m} \right) \quad (2)$$

with  $\mathbf{p}_1 = \mathbf{p}_i$ ,  $\mathbf{p}_2 = \mathbf{p}_i - mgT$ ) and if the laser phases  $\phi_1^0, \phi_2^0$  verify  $\phi_1^0 = \phi_2^0$ . If these conditions are fulfilled, and if the sample coherence length  $w$  is much larger than the final wave-packet separation  $|\mathbf{r}_{f,a} - \mathbf{r}_{f,b}|$  - or equivalently if the Doppler width  $k\Delta p/m$  experienced by the travelling atoms is much smaller than the frequency  $1/T$  -, one obtains an almost fully constructive interference in the excited state. The succession of two  $\pi/2$  pulses then mimics very efficiently a single  $\pi$  pulse, the quantum channel to the lower state being shut off by destructive interferences.

This compensation of the phase induced by the external atomic motion through fine-tuned laser phases is at the heart of our proposal. A key point is that condition (1), expressing the equality of the quantity  $I = -\mathbf{p}_f \cdot \mathbf{r}_f + S + \hbar\phi$  for both paths, is independent of the initial wave-packet position. Identical conditions on the pulse frequencies and frequency ramp thus prevail to obtain the full population transfer for a group of atomic wave-packets with a common average momentum and internal state. This property will allow to address simultaneously the numerous wave-packets generated in the  $\pi/2$  pulse sequence.

Applying a second sequence of two  $\pi/2$  pulses with downward wave-vectors [15], one obtains a vertical Bordé-Ramsey interferometer bent by the gravity field sketched on Fig. 2 Starting with a sufficiently coherent sample in the lower state state, and with well adjusted frequencies (2) and ramp slopes, the previous discussion shows that a net momentum transfer of  $2\hbar\mathbf{k}$  is provided to each atom during the interferometric sequence. For the special interpulse duration

$$T := T^0 = \frac{\hbar k}{mg}, \quad (3)$$

these atoms end up in the lower state with their initial momentum. Two major benefits are then expected. First, the periodicity of the sample motion in momentum gives rise to levitation. Second, only two frequencies, given by (2), are involved in the successive resonant pairs of  $\pi/2$  pulses. In particular, the first and the fourth pulse of the Bordé Ramsey interferometer, as well as the second and the third one, correspond to identical resonant frequencies:  $\omega_1^0 = \omega_4^0$  and  $\omega_2^0 = \omega_3^0$ .

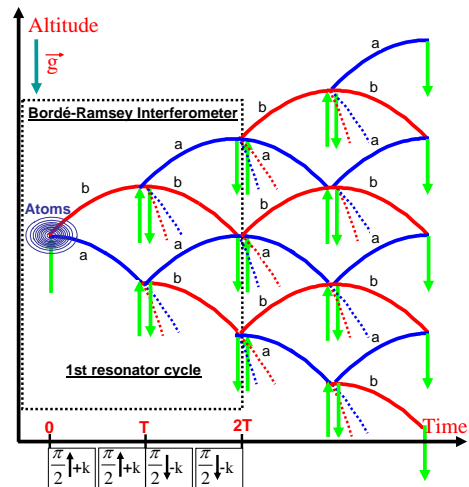


FIG. 2: Levitating atomic trajectories in the sequence of pulses. The first four pulses generate a vertical Bordé-Ramsey interferometer. The central positions of the wave-packets explore a network of paths which doubles at each laser pulse.

If the previous conditions are fulfilled, the repetition of the interferometer sequence gives rise to a network of levitating paths - sketched on Fig. 2 - reflecting the diffusion of the atomic wave in the successive light pulses. The same laser field is used to levitate the sample and to perform its interrogation, generating a clock signal based on either one of the two frequencies  $\omega_1^0, \omega_2^0$ . Our measurement indeed rests on the double condition (2, 3), which must be fulfilled to ensure this periodic motion: should the parameters  $(T, \omega_{1,2,3,4})$  differ from their resonant values  $(T^0, \omega_{1,2,3,4}^0)$ , the outgoing channels would open again and induce losses in the levitating cloud, which can be tracked by a population measurement. We expect multiple wave interference to induce a narrowing of the resonance curve associated with the levitating population around this condition.

We consider a free-falling diluted sample, taken at zero temperature and described initially by a macroscopic Gaussian wave-function. In-between the pulses, the propagation of a Gaussian wave-packet is amenable to a change of its central position and momentum according to classical dynamics, of its widths according to  $w_{x,y,z}^2(t) = w_{x,y,z0}^2 + \frac{\hbar^2}{4m^2w_{x,y,z0}^2}(t - t_0)^2$ , and to the addition of the action phase already considered [16]. Since the light pulses are short, their action onto each atomic wave-packet is efficiently modeled by a position-dependent Rabi matrix [17] evaluated at the packet center. The evolution of each wave-packet is thus very simple. However, their number doubles at each light pulse, which makes their book-keeping a computational challenge. This difficulty, intrinsic to the classical simulation of an entangled quantum state, has limited our investigation to a sequence of sixteen pulses, involving 28 levitating Bordé-Ramsey interferometers associated with the

resonant paths and a total number of  $N \simeq 64000$  atomic waves sufficient to probe the expected multiple wave interference effects.

The atomic transition used in this setup should have level lifetimes longer than the typical interferometer duration (ms), and the atoms should be cooled at a sub-recoil temperature in order to keep a sufficient levitating population in spite of the momentum filtering realized by the successive interferometers. Possible candidates are the  $^{87}\text{Sr}$ , Yb and Hg atoms, which have a narrow clock transition in their internal structure. To guarantee a sufficient overlap of the interfering wave-packets, we consider a cloud of coherence length  $w = 100 \mu\text{m}$  much larger than the wave-packets separation on the order of  $d \simeq 15 \mu\text{m}$ . The  $\pi/2$  pulses have a Rabi pulsation of  $\Omega = 2\pi \times 10^5 \text{Hz}$ . Fig. 3 shows the levitating and the falling atomic population in the lower state as a function of the frequency shift  $\delta\omega$  from the resonant frequencies  $\omega_{1,2,3,4}^0$ . It reveals a fully constructive interference in the levitating arches when the resonance conditions are fulfilled, as well as the expected narrowing of the central fringe associated with the levitating wave-packets. Falling wave-packets yield secondary fringe patterns with shifted resonant frequencies, which induce an asymmetry in the central fringe if the total lower state population is monitored. This effect, critical for a clock operation, can nonetheless be efficiently attenuated by limiting the detection zone to the vicinity of the levitating arches. This strategy improves as the levitation time increases: the main contribution to the “falling” background comes then from atoms with a greater downward momentum and thus further away from the detection zone. Besides, multiple wave interferences sharpen the symmetric “levitating” central fringe fast enough to limit the effect of the asymmetric background of falling fringes. Considering a shift  $\delta T$  from the resonant duration  $T_0$ , one obtains also a central fringe narrowing as the number of pulses increases.

To keep the sample within the laser beam diameter, it is necessary to involve a transverse confinement, which may be obtained by using laser waves of spherical wave-front for the pulses [10]. In contrast to former horizontal clocks [5], the atomic motion is here collinear to the light beam, which reduces the frequency shift resulting from this wave-front curvature. A weak-field treatment, to be published elsewhere, shows that this shift is proportional to the ratio  $\Delta\omega_{curv} \propto k \langle v_{\perp}^2 \rangle T / R$ , involving the average square transverse velocity  $\langle v_{\perp}^2 \rangle$  and the field radius of curvature  $R$  at the average altitude of the levitating cloud. An other key point is that the central fringe sharpens fast as the condensate experiences these first interferometers, which confirms the accuracy improvement expected for both the frequency and acceleration measurement through multiple wave interference.

An analysis of the atomic motion in momentum space, sketched in the energy-momentum diagram of Fig. 4, is especially enlightening. In this picture, the total energy accounts for the rest mass, the kinetic and the gravita-

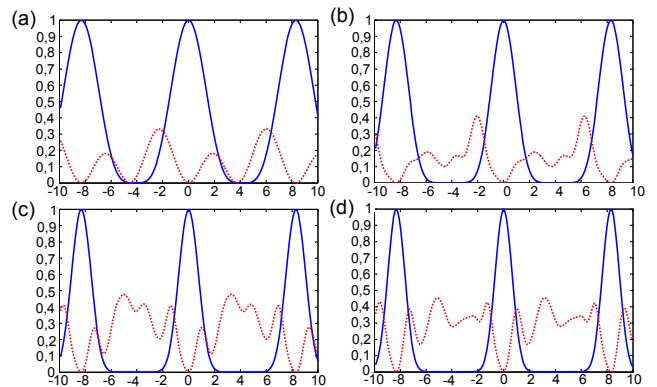


FIG. 3: Fraction of the total sample population levitating (full line) and falling (dashed line) in state  $a$  after one, two, three and four pulse sequences as a function of the frequency detuning  $\delta\omega$  (kHz) ( $\omega_{1,2,3,4} := \omega_{1,2,3,4}^0 + \delta\omega$ ) and for a resonant interferometer duration  $2T^0$ .

tional potential energy. It is a parabolic function of the momentum. Each star stands for a specific wave-packet, the motion of which between the light pulses is represented by horizontal dashed arrows, in accordance with energy conservation. For the duration  $T := T^0$ , and for a sufficiently coherent atomic sample, Fig. 4 reveals that the atomic motion in momentum is periodic and bounded between two well-defined values associated with the photon recoil. The momentum confinement is here provided by destructive interferences which shut off the quantum channels going out of this bounded momentum region. This remarkable property suggests an analogy with a resonator in momentum space. Following this picture, we have computed the lower-state wave-function after  $N$  resonant pulse sequences of duration  $2T_0$ , considering only the vertical axis with no loss of generality. Each wave-packet ends up at rest, and with a momentum dispersion  $\Delta p_f$ . Applying the phase relation (1) successively between the multiple arms, one obtains:  $\psi_a(p, t_0 + 2NT_0) = C_N e^{-\frac{p^2}{\Delta p_f^2}} \sum_{Paths} e^{-iz_f p}$ .  $C_N$  is a complex number, and the altitudes  $z_f$  are the endpoints of the resonant paths drawn on Fig. 2, on which the sum is performed. By labeling these paths with the instants of momentum transfer, this sum appears up to a global phase as an effective canonical partition function of  $N$  independent particles, with  $Z_1 = 2 \cos^2(kT p / 2m)$  the one-particle partition function. This yields a wave-function of the form  $\psi_a(p, t_0 + 2NT_0) = C'_N e^{i\phi(\mathbf{p}, N)} e^{-\frac{p^2}{\Delta p_f^2}} \cos^{2N}(p/p_m)$ , with  $p_m = 2m/kT_0$ . As  $N \rightarrow +\infty$ , multiple wave interferences thus yield an exponential momentum localization, scaled by the momentum  $p_m$ , around the rest value  $p = 0$ . The diffusion in altitude observed in the network of paths of Fig. 2 reflects a back-action of this localization.

To summarize, we have proposed a space-time atomic sensor achieving the levitation of an atomic sample through multiple wave interference effects in a series of

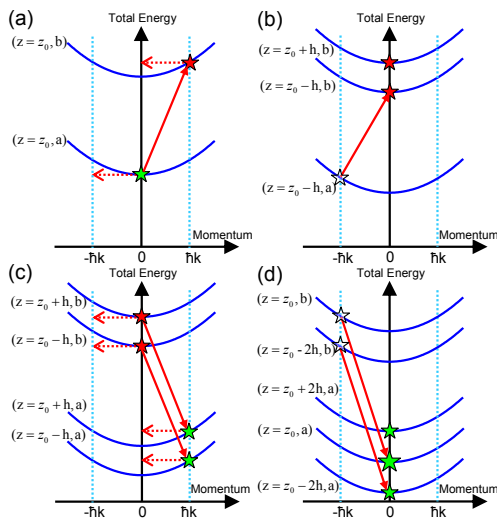


FIG. 4: Motion of the atomic wave-packets in the energy-momentum picture for the interferometer duration  $2T^0$ . Figs. (a,b,c,d), associated with the 1st,2nd,3rd and 4th light pulses respectively, show the packets present in coherent superposition (full stars) immediately after - or transferred (transparent stars) during - the considered pulse, whose effect is represented by a full red arrow.

vertical  $\pi/2$  light pulses. The sensitivity of this levitation towards a double resonance condition can be used to realize a frequency or an acceleration measurement, with an accuracy improving with the number of interfering wave-packets. The sample needs to be cooled at a subrecoil temperature in order to yield the desired interference effects. For a sufficiently diluted cloud, transverse confinement may be provided by the wave-front of spherical light pulses. This system involves no off-resonant trapping light field and is thus exempt from the corresponding frequency shifts. It appears as a promising alternative to current optical-lattice clocks [1] and cold atom gravimeters [18]. It may also operate as an atomic gyrometer [4, 19] by tilting the lasers or by introducing additional horizontal light pulses, and exploiting the generated horizontal wave-packet motion. As exposed, this setup is a passive resonator in momentum space, it could nonetheless also be turned into an active system through matter-wave amplification by plunging the levitating wave-packets into a reservoir of source atoms.

The authors are grateful to S. Bize, P. Bouyer, A. Clairon, A. Landragin, P. Lemonde and Y. LeCoq for stimulating discussions. F. Impens thanks N. Zagury and L. Davidovich for hospitality. This work is supported by CNRS and DGA (Contract No 0860003). SYRTE and L.P.L. are affiliated with IFRAF(www.ifraf.org).

- 
- [1] A. D. Ludlow et al., *Science* **319**, 1805 (2008); R. L. Targat et al. *Phys. Rev. Lett.* **97**, 130801 (2007); M. Takamoto et al. *J. Phys. Soc. Jpn.* **75**, 104302 (2006).
- [2] S. Blatt et al., *Phys. Rev. Lett.* **100**, 140801 (2008); T. Rosenband et al., *Science* **319**, 1808 (2008).
- [3] C. J. Bordé et al. *Phys. Rev. A* **30**, 1836 (1984).
- [4] C. J. Bordé, *Phys. Lett. A* **140**, 10 (1989).
- [5] G. Wilpers et al., *Metrologia* **44**, 146 (2007).
- [6] T. Trebst et al. *IEEE Trans. on Inst. and Meas.* **50**, 535 (2001).
- [7] H. Katori et al., *Phys. Rev. Lett.* **91**, 173005 (2003).
- [8] M. Weitz, T. Heupel, and T. W. Hänsch, *Phys. Rev. Lett.* **77**, 2356 (1996); H. Hinderthür et al., *Phys. Rev. A* **59**, 2216 (1999); T. Aoki et al., *Phys. Rev. A* **67**, 053602 (2003).
- [9] M. Wilkens et al., *Phys. Rev. A* **47** (1993).
- [10] F. Impens, P. Bouyer, and C. J. Bordé, *Appl. Phys. B* **84**, 603 (2006).
- [11] C. J. Bordé and F. Impens, in *Abs. of ICOLS 2007*. [www.laserspectroscopy.org](http://www.laserspectroscopy.org), (2007); F. Impens et. al. in *Abs. of YAO 2007* (2007)
- [12] This assumption does not induce any loss of generality: the following discussion would also apply to any mode of the Hermite-Gauss basis, and thus to any wave-function by linearity.
- [13] This equation can also be interpreted as a generalized optical path in 5D [14].
- [14] C. J. Bordé, in *Proc. of the Enrico Fermi International School of Physics*, **168** (2007), and *Eur. Phys. Jour. D* in press.
- [15] In the configuration of Fig. 2, the two pulse pairs are performed successively, which maximizes the interferometric area for a fixed interferometer duration; one could nonetheless also let a finite time between them.
- [16] C. J. Bordé, *Metrologia* **39**, 435 (2001).
- [17] C. J. Bordé, in *Atom Interferometry* (Ed. P. R. Berman, 1997).
- [18] A. Peters, K. Y. Chung, and S. Chu, *Nature* **400**, 849 (1999).
- [19] B. Canuel et al., *Phys. Rev. Lett.* **97**, 010402 (2006), and references therein.